SU-SEL-64-105

Radar Astronomy of Solar System Plasmas

by

Von R. Eshleman

August 1964

Scientific Report No. 4

Prepared under
National Aeronautics and Space Administration
Research Grant No. NsG-377

RADIOSCIENCE LABORATORY

STANFORD ELECTRONICS LABORATORIES

STANFORD UNIVERSITY • STANFORD, CALIFORNIA

SEL-64-105

RADAR ASTRONOMY OF SOLAR SYSTEM PLASMAS

By

Von R. Eshleman

August 1964

Scientific Report No. 4

Prepared under
National Aeronautics and Space Administration
Research Grant No. NsG-377

Radioscience Laboratory
Stanford Electronics Laboratory
Stanford University Stanford, California

CONTENTS

ILLUSTRATIONS

ABSTRACT

Harmonic-frequency radar echoes from the moon are being used at Stanford to measure the density and dynamics of the ionized cislunar medium by a combination of Doppler frequency (phase path) and Faraday polarization techniques. For example, during the solar eclipse of July 20, 1963, comparisons of the radar data with ionosonde and VLF whistler measurements appear to indicate that at Stanford, where the maximum solar disk area covered by the moon was 23 percent, the radar detected a blocking of the solar wind by the moon.

The deep space probes Pioneer A and B, which are due to be launched in the spring and summer of 1965, will carry receivers for radio propagation studies of the interplanetary medium. Harmonic, modulated, circularly-polarized signals at 50 and 425 Mc will be transmitted from Stanford to the probes, where measurements of the phase path, group path, and polarization will be made. Sensitivities correspond to the ability to measure the average interplanetary volume density of electrons to an accuracy of 0.5 cm^{-3} when the probe is at its maximum distance. Changes of average electron density can be detected which are as small as 0.005 cm^{-3}. One or both of the spacecraft may be fired on a trajectory such that it will be occulted by the moon, so that measurements on the amplitudes of the two signals, as they are cut off by the limb of the moon, can give a sensitive measure of a possible lunar ionosphere.

Theoretical studies have been made of radio propagation through planetary ionospheres and atmospheres. It appears that a particularly simple and menaingful measurement technique would involve radio wave propagation at two or more frequencies between the earth and a space probe which is occulted by the planet. As the ray paths pass nearer and nearer the limb of the planet, refraction in the ionosphere and atmosphere, and diffraction at the limb, make possible sensitive measures of the electron density profile in the ionosphere and the neutral density profile of the atmosphere. An experiment of this type is planned for the Mariner C missions of 1964-65.

Continuing radar studies of the sun by the Lincoln Laboratory of MIT show an outward flow of plasma at the reflecting level, and a large amount of Doppler spread due to turbulence. The effective radar cross section of the sun is highly variable from day to day. When space probes which can be sent behind the sun become available, occultation measurements somewhat akin to the planetary studies described above could augment the ground-based radar studies to help define the density, structure, and dynamics of the inner and outer coronal regions of the sun.

1. INTRODUCTION

The subject of this paper is the study, by radar techniques, of gaseous regions in the solar system. The interplanetary medium, the solar corona, and planetary atmospheres and ionospheres are considered. The past experimental results are reviewed, although much of the discussion is of immediate plans for, and future potentialities of, this method of investigating the solar system.

Most of the regions of interest contain gases which are wholly or partially ionized, so that the radar techniques of study involve propagation of electromagnetic waves in a plasma. However, a consideration of propagation in non-ionized portions of planetary atmospheres is also included since, under certain conditions, both atmospheric and ionospheric perturbations to the radar waves will be important.

The atmosphere and ionosphere of the earth are considered here only with respect to their effects on the measurements of more distant regions.

Both monostatic and bistatic radar astronomy techniques are discussed. Here these terms are meant to imply that either transmitter and receiver are both on the earth or both on a space probe (monostatic), or one is on the earth and the other on a space probe (bistatic). The term "radar" is used here to include conditions where there may be nearly straight-line propagation from a transmitter to a receiver, as well as circumstances where the propagation path includes reflection from a relatively discrete target.

The subject matter of this chapter is sometimes referred to as "soft-target" radar astronomy to differentiate it from "hard-target" radar studies of the surfaces of the moon, planets, satellites, and asteroids.

2. FIRST-ORDER THEORY

A first-order set of formulas will be presented to illustrate several of the effects which are amenable to measurement by radar techniques. The aim will be to concentrate more on the techniques as they relate to astronomical studies of the solar system, rather than on the full details of the theory, so that only a simplified set of equations is given.

The refractive index n of a collisionless plasma in the absence of a static magnetic field is real and independent of wave polarization:

$$n = \left(1 - \frac{f_o^2}{f^2}\right)^{\frac{1}{2}} = \left[1 - \left(\frac{c^2 r_e}{\pi}\right)\frac{N_e}{f^2}\right]^{\frac{1}{2}} \qquad (1)$$

where rationalized MKS units are used, f is the wave frequency, f_o is the plasma frequency, $c \cong 3 \times 10^8$ m/s, $r_e = 2.8178 \times 10^{-15}$ m, the classical electron radius, and N_e is the electron volume density. For the case of a uniform and relatively dilute electron gas, where $f \gg f_o$,

$$\Delta v = v_\phi - c = \frac{c}{n} - c = c - v_g = c - cn \cong \frac{c^3 r_e N_e}{2\pi f^2} \quad \text{m/s} \qquad (2)$$

Thus Δv is the amount by which the phase velocity exceeds c and also the amount by which c exceeds the group velocity.

If the integrated electron density (columnar electron density) is I electrons/m^2 for a path of length D, then a wave packet after propagating at v_g over the distance D will be displaced by a distance R behind where it would have been in free space. The amount is $\Delta vD/c$ meters, or since $N_e D = I$,

$$R = \left(\frac{c^2 r_e}{2\pi} \right) \frac{I}{f^2} \quad \text{meters} \tag{3}$$

The dimensional constant $(c^2 r_e/2\pi)$, which will be encountered in several formulas, has the well-known value of $80.6/2$ or $40.3\ m^3/s^2$.

Other simple arguments such as used above show that the frequency of the wave after propagating through the distance D will be different from the initial frequency if I is changing with time. To first order, and assuming no relative motion of transmitter and receiver,

$$f_{DE} = \left(\frac{c^2 r_e}{2\pi} \right) \frac{I_t}{cf} \quad \text{cycles per second} \tag{4}$$

where $I_t \equiv dI/dt$ and f_{DE} is the apparent Doppler frequency, or "Doppler excess", due to the changing density. The Doppler frequency due to path length change would be additive to this effect.

For quasi-longitudinal propagation when there is a weak $(f >> f_L)$ static magnetic field in the dilute plasma, there will be a Faraday rotation of the plane of polarization of the wave given by

$$\Omega = \left(\frac{c^2 r_e}{2\pi} \right) \frac{f_L I}{cf^2} \quad \text{cycles} \tag{5}$$

where f_L is the longitudinal gyro frequency. If the plasma is characterized by a collision frequency ν, due to electron-neutral or other types of collisions, then the wave amplitude will vary according to $\exp(-\tau)$, where

$$\tau = \left(\frac{c^2 r_e}{2\pi} \right) \frac{\nu I}{c f^2} \qquad \text{nepers} \tag{6}$$

While the statements above were made for a homogeneous medium, they apply equally well if there are electron density gradients in the direction of propagation, as long as $f \gg f_o$ at all positions and the gradients are sufficiently gentle to prevent sensible reflections. If both N_e and f_L or ν vary in the longitudinal direction, then $f_L I$ and νI in (5) and (6) should be determined by integration.

For transverse gradients in the electron density, the direction of propagation changes away from the gradient. The amount of change in the direction of propagation is

$$\beta = -\left(\frac{c^2 r_e}{2\pi} \right) \frac{I_x}{f^2} \qquad \text{radians} \tag{7}$$

where $I_x \equiv dI/dx$, and the x-direction is the direction of the maximum gradient in the plane transverse to the direction of propagation.

If in (7) β is a function of x, then the amplitude of the wave will change due to focussing. If the rays do not form caustics and the region of ray bending is localized, then the logarithmic gain G of a plane incident wave due to the focussing would be

$$G = -\frac{1}{2} \ln \left(1 + y \frac{d\beta}{dx} \right) \simeq \left(\frac{c^2 r_e}{2\pi} \right) \frac{y I_{xx}}{2 f^2} \qquad \text{nepers} \tag{8}$$

where $I_{xx} \equiv d^2 I/dx^2$ and y is the distance from the focussing region to the receiver. The extension of this formula to possible two-dimensional focussing is straightforward.

Many phenomena of interest in radar studies of solar system plasmas are adequately described by the above first-order formulas. There are important exceptions, of course, and these will be mentioned as encountered in the later sections.

For the case of non-ionized planetary atmospheres, the refractive index of the gas is $n = 1 + 10^{-6} N$, where N is the refractivity in the commonly used N-units. For a gas consisting of a mixture of non-polar molecules,

$$N = \sum_n \frac{\alpha_n p_n}{T} \tag{9}$$

where the α_n are constants for the constituent gases, the p_n are their partial pressures, and T is the absolute temperature. For polar molecules such as water vapor, there is an extra term varying as p_n/T^2.

Since the refractive index for non-ionozed gases is greater than unity and not a function of wavelength at the radio wavelengths of interest here, $v_\phi = v_g < c$. Thus there is equal phase and group retardation and there is ray bending in the direction of the transverse gradient of density. There is little absorption for the atmospheres and wavelengths of interest here, and there are no anisotropic and doubly refractive effects.

The refractivity of an ionized gas corresponding to the conditions of (1) can be expressed in N units as

$$N = -10^6 \left(\frac{c^2 r_e}{2\pi} \right) \frac{N_e}{f^2} \tag{10}$$

if also $f >> f_o$. Conversely, (3), (4), (7), and (8) could be used for a non-ionized gas by replacing I by

$$\pm 10^{-6} \left(\frac{2\pi}{c^2 r_e} \right) NDf^2 \tag{11}$$

where the plus sign should be used in (3) while the minus sign should be used in (4), (7), and (8).

3. THE CISLUNAR MEDIUM

Monostatic (earth-based transmitters and receivers) radar echoes from the moon have been used to study the ionized regions between the earth and the moon. Since our principal concern here is in regions beyond the earth's ionosphere and magnetosphere, we will not review the extensive moon-echo results which are based only on Faraday polarization measurements, since from (5) these are sensitive only to the near-earth regions where the magnetic field strength is relatively high. To sense the ionization in the absence of a magnetic field, it is convenient to use methods corresponding to (3) or (4). These might then be included with polarization measurements to help make a separate determination of ionization near the earth and the ionization in the remaining cislunar medium.

Moon-radar work of this type is being conducted at Stanford[1,2,3]. Since early 1962, about 400 hours of Doppler data corresponding to (4) have been obtained. In addition, about 100 hours of this time includes data on polarization rotation (eq. 5) and its rate of change with time. Amplitude data was taken for much of this time so that an analysis of focussing (eq. 8) can be made. A new technique based on pulse-compression is just now being initiated in an attempt to measure the group delay (eq. 3).

The radar system consists of two transmitters and two antennas. A 300-kw transmitter at 25 Mc is used with an array of 48 log-periodic antenna elements arranged in two 1200-foot north-south rows. A 50-kw transmitter at 50 Mc is used with a steerable 150-foot diameter parabolic antenna. Simultaneous operation of the two systems is possible for about two hours per day, this limit being set by the azimuthal beamwidth of the log-periodic array.

In practice, the use of two frequencies affords self-calibration which often marks the difference between a relatively simple experimental procedure and one which is very difficult or impossible to implement. If the two frequencies are f and nf with $n > 1$, and Δ is used to indicate the conditions at f minus those at nf; then

$$\frac{\Delta R}{R} = \frac{f_{DD}}{f_{DE}} = \frac{\Delta\Omega}{\Omega} = \frac{\Delta\tau}{\tau} = \frac{\Delta\beta}{\beta} = \frac{\Delta G}{G} = \frac{n^2 - 1}{n^2} \qquad (12)$$

In (12), f_{DD} is the frequency difference of the received lower frequency and 1/n of the received higher frequency. Thus by measuring this frequency, or the difference in delay of the two pulses, or the difference in the received polarization at the two frequencies, etc., then the total Doppler excess, pulse delay, Faraday rotation, etc., for the lower frequency can be found from knowledge of n.

While the main interest is in regions beyond the ionosphere and magnetosphere, it is now clear that most of the observed effects are due to changes which take place near the earth. Doppler excess measurements made at different times of day show the expected morning increase and evening decay of ionospheric electron density, together with irregularities in the ionosphere that become more pronounced during magnetic storms. Figure 1 illustrates several of these effects. In the top curve are shown Doppler excess measurements averaged over one-minute intervals for a two-hour period during the late morning of March 4, 1962. The bottom curve is the integral of the top curve, showing the relative value of I as a function of time for the cislunar medium, where most of the change probably occurred in the ionosphere. The fluctuations of Doppler excess, with periods from a few to about 30 minutes, indicate changes similar to those found in measurements of ionos-

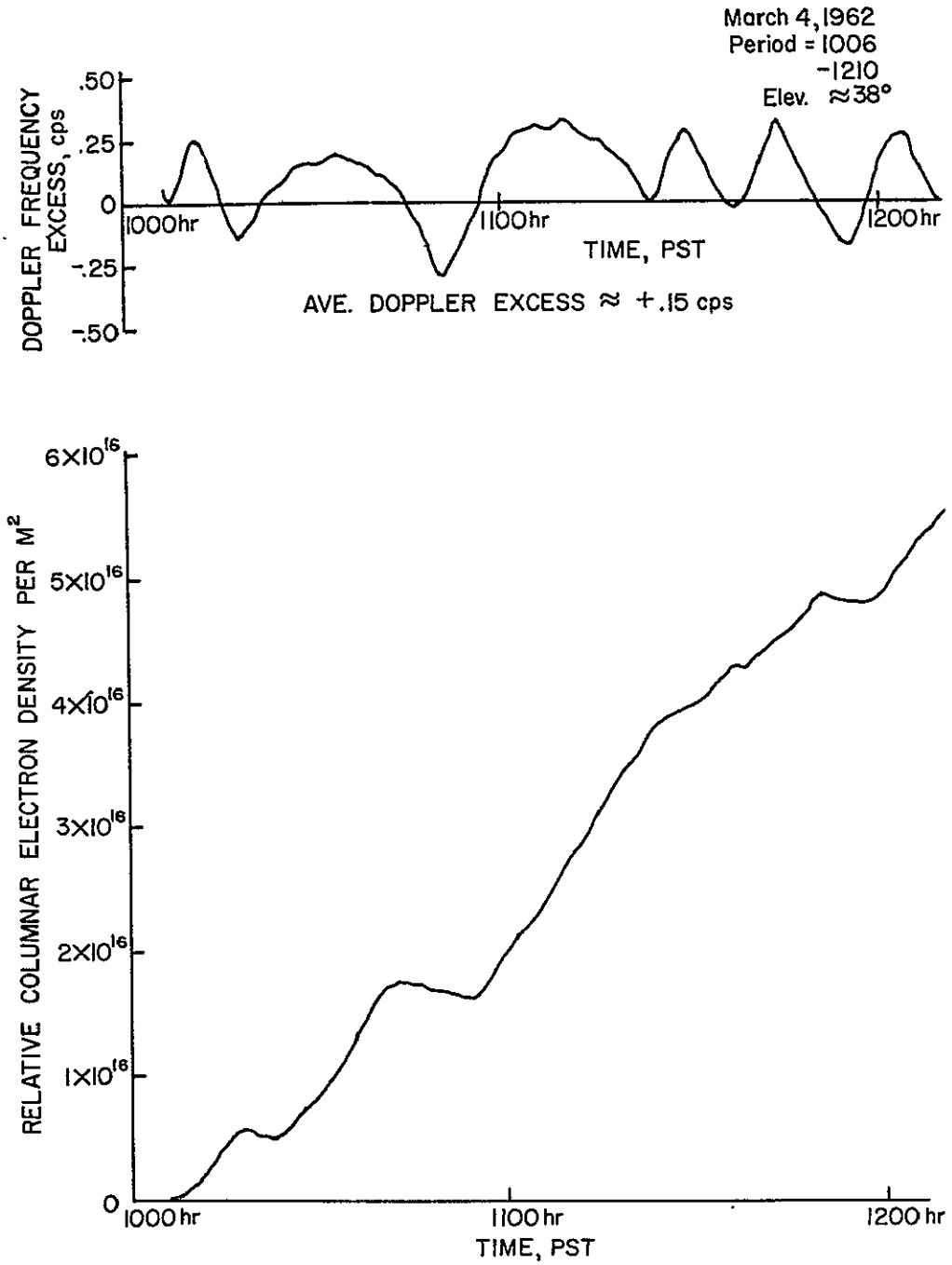

Fig. 1 SMOOTHED DOPPLER EXCESS FREQUENCY (a) AND ITS INTEGRAL (b) SHOWING THE CHANGING ELECTRON DENSITY BETWEEN THE EARTH AND THE MOON

pheric content by Evans and Taylor[4] using the Faraday moon-radar technique, and they are presumably due to large-scale ionospheric irregularities (see, for example, Little and Lawrence[5]).

Simultaneous measurements of Doppler excess and of Faraday polarization at 25 Mc and 50 Mc have been used in an attempt to separate near-earth effects from changes which may take place in the interplanetary medium between the magnetospheric boundary and the moon. In principle, the value of I determined from Doppler measurements includes both regions while I determined from Faraday polarization only includes near-earth ionization, so that their difference is a measure of effects in the interplanetary medium.

However, in the polarization technique it is necessary to compute from an assumed N_e height profile a weighted average value of f_L along the propagation path in order to compute I from a measurement of Ω. For studies of the ionosphere itself, this problem causes little difficulty since the bulk of the ionospheric ionization of interest exists between narrow height limits where the value of f_L varies very little. However, if we are looking for effects well away from the earth which may be only a small fraction of the near-earth effects, then it becomes necessary to have relatively precise electron density profile information for both the ionosphere and magnetosphere. The magnetospheric region above several thousand kilometers but below the magnetospheric boundary at 60,000 or more kilometers appears to have an integrated electron content comparable to that of the ionosphere[6]. This magnetospheric content has a much smaller diurnal variation than the ionosphere, although it is markedly affected by magnetic storms.

It now appears that the combined Faraday-Doppler measurements are turning up new effects of interest in terms

of the changing electron density profile in and between the ionosphere and magnetosphere, but that the detection of effects beyond the magnetosphere may be relatively infrequent. A major exception to this statement may be the measurements that were taken during the solar eclipse of July 20, 1963.

The Faraday data taken on the eclipse day shows the type of ionospheric reduction in content that was expected. This will not be discussed further. Figure 2 shows the difference of the relative integrated density as determined by the Doppler method and as determined by the Faraday method for the earth-moon path on the eclipse and adjacent days. Figures 2a, c, d show the results for the control days, July 19, 21, and 22. Figure 2b is a similar curve for the eclipse day; it also includes the optical obscuration curve and a theoretical curve explained below. The electron content difference curve shows an unusually large decrease during the eclipse, reaching a low value soon after maximum obscuration and staying near this value for the remaining 1.5 hours of measurement. The total change during the measurement period was about 2.8×10^{16} electrons m^{-2}.

It is unfortunate that only about four hours of data could be obtained, since it appears that large changes beyond the ionosphere were already occurring at the start of measurements, and nothing was detected of a possible recovery phase. The change on the eclipse day was greater than on any of the control days, although an important change beyond the ionosphere was observed on the day after the eclipse. The magnetic A_p index for July 21 was 26, as compared with 5, 6, and 13, for July 19, 20, and 22, respectively. From the relative intensity and time of the effect noted on July 20, it appears to be associated with the eclipse, although the location and cause of the change cannot as yet be specified.

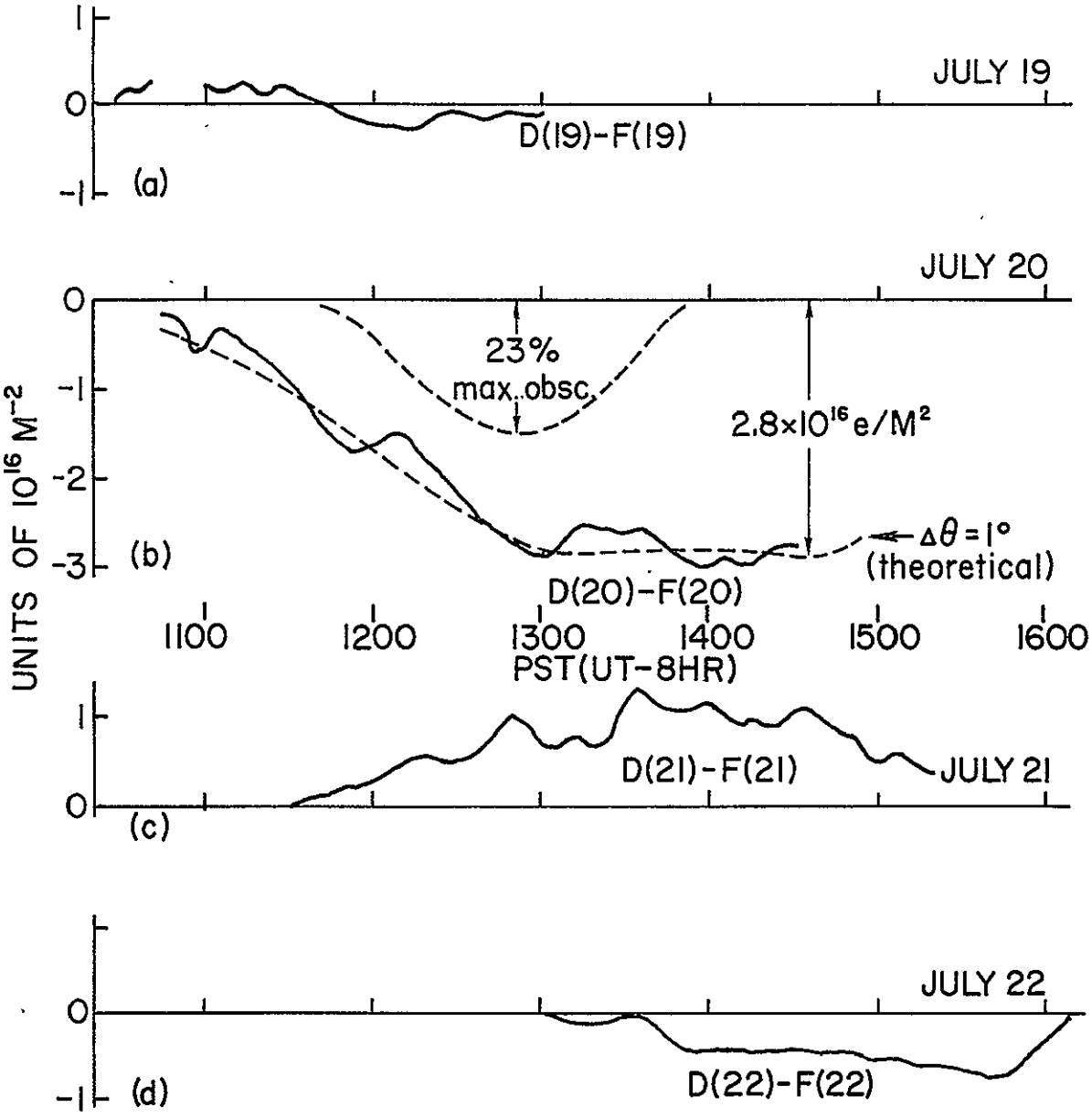

Fig. 2 CHANGES IN ELECTRON DENSITY BEYOND THE IONOSPHERE MEASURED BY COMBINED FARADAY AND DOPPLER TECHNIQUE: (a) July 19; (b) Eclipse Day, July 20. Also shown (dotted line) is the optical obscuration of the sun and the theoretical integrated density in the lee of the moon for a solar wind dispersion of $\Delta\theta = 1°$; (c) July 21; (d) July 22.

One possible interpretation of the effect observed during the eclipse is that there is a region of decreased solar wind density in the lee of the moon. That is, the particles in the wind flowing outward from the sun are absorbed or deflected by the moon, causing a decreased density behind it. The amount and extent of this decrease depend on the spread in direction of particle velocities. A large spread will give a small decrease of modest extent, while a small spread (all particles coming almost directly from the sun) will give almost complete depletion, extending great distances behind the moon. Figure 3 shows a calculated density distribution in this region for a Gaussian spread in particle velocity direction of $\Delta\theta = 2°$. The integral of this density between the earth and moon would be the quantity measured by the Doppler-Faraday technique. In Figure 2b such an integral has been plotted for $\Delta\theta = 1°$ and its shape shows reasonable agreement with the limited eclipse-day data.

One difficulty with the solar wind interpretation is that the total decrease in density amounts to about 75×10^{6} m^{-3} averaged over the cislunar path, which implies a solar wind density of 10^{8} m^{-3} (100 cm^{-3}). This density is nearly an order of magnitude greater than the proton densities measured by the Mariner 2 space probe[7] which, however, was not sensitive to low-velocity particles.

A second difficulty is that the motion of the earth and moon about the sun should cause the particle shadow of the moon to be tilted in a direction opposite to this motion. For the maximum density change to occur near the time of visual occultation requires that the solar wind retain sufficient angular momentum form the sun's rotation so that its tangential velocity is approximately equal to the earth's orbital velocity. If this were not so, and the particles moved directly radially from the sun, the change

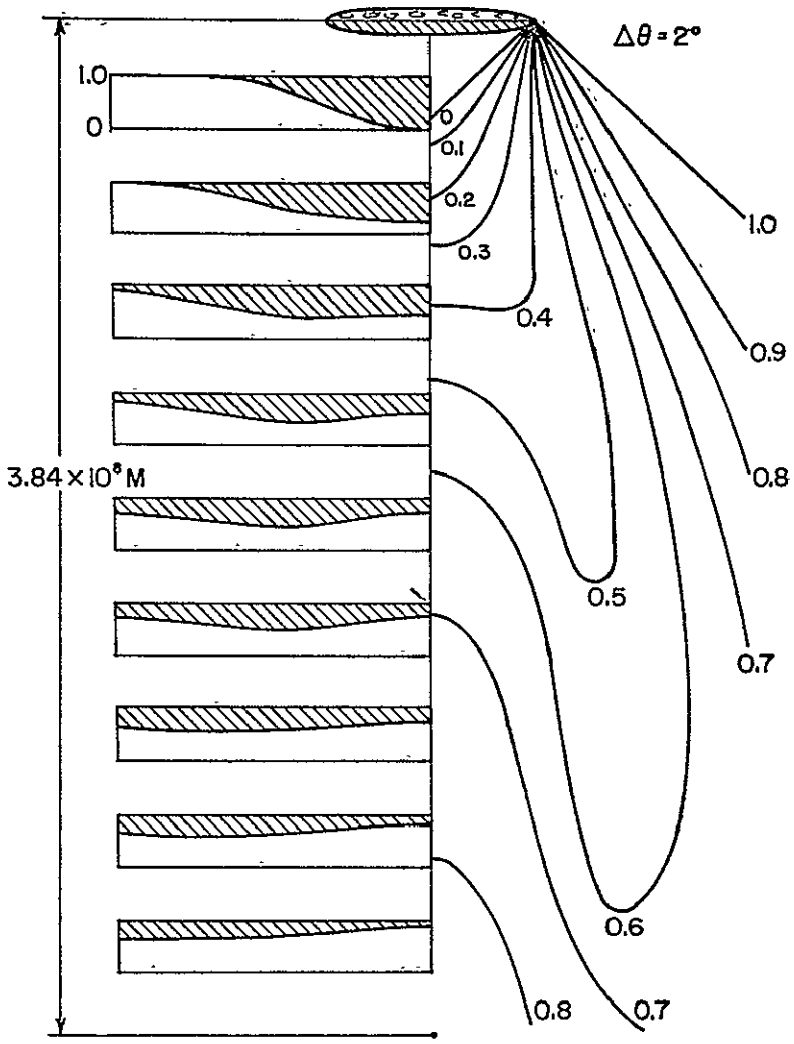

Fig. 3 CALCULATED ELECTRON DENSITY IN THE LEE OF THE MOON WITH A SOLAR WIND DISPERSION OF $\Delta\theta = 2°$. On the left is shown the normalized density as a function of distance from the moon-earth line at various distances behind the moon. On the right is shown the contours of constant electron density in the same region. The horizontal scale is greatly expanded.

should have occurred about eight hours earlier.

Another possibility is that this density change occurred within the magnetosphere, as discussed above. Whistler analyses made at Stanford, however, show little magnetospheric change during this time[8]. Also, if the eclipse was responsible for changes in the magnetosphere, the only immediately obvious mechanism would be an effect related to the moon's blocking of the solar wind. However, the shape and time of occurrence of the depression require the same narrow velocity dispersion and tangential velocity component in the solar wind as described above.

Future possibilities for radar studies of the cislunar medium include the use of lunar orbiting spacecraft and transmitters or transponders on the lunar surface. It has been proposed by Stanford that AIMP (anchored interplanetary monitoring platform) spacecraft which will be orbited around the moon transmit at a subharmonic of the telemetry frequency. Both frequencies could then be monitored on the earth for Doppler excess and group path measurements. Such measurements would be more precise than are possible with lunar radar techniques since reflection from the rough moon limits the accuracy of frequency, time delay, and amplitude measurements. The AIMP measurements would be particularly interesting when the propagation path is along the direction of the solar-wind wake of the earth or moon. If other measurements are made at the same time of the ionospheric and magnetospheric profile (with topside sounders, a geostationary or highly elliptical earth satellite, or incoherent scatter radar), it should be possible to obtain information on the interplanetary density near the earth-moon system, and the wake these bodies make in the solar wind.

The proposed radio propagation experiment for these spacecraft includes bistatic radar studies of the lunar

surface and occultation measurements of a possible lunar atmosphere or ionosphere.

4. THE INTERPLANETARY MEDIUM

To keep the near-earth plasma from masking effects of the interplanetary medium, it is obvious from the above discussion that longer propagation paths than to the moon are desirable. Monostatic radar echoes from the planets could in principle be used, but the radar system requirements for such a study would be difficult to achieve. Low frequencies are desired because most of the effects of interest vary as f^{-2}, but because of the increase in cosmic noise and the lessening of antenna gain per unit aperture as frequency is lowered, extremely high transmitter power would be required. With planetary echoes there would also be the difficulty of having ionospheres to contend with at both ends of the path[9].

The Center for Radar Astronomy at Stanford University and the Stanford Research Institute is preparing a radio propagation experiment for the Pioneer A and B spacecraft. It is planned that these probes will be launched into interplanetary space in the spring and summer of 1965. Other experiments are designed for measurements of the magnetic field, the local interplanetary plasma, cosmic rays, and micrometeorites.

The radio propagation (bistatic radar) experiment involves transmissions from Stanford at 50 and 425 Mc and reception in the space probes. Transmitter powers are a continuous 300 kw at 50 Mc and 30 kw at 425 Mc. Both will be connected to the steerable 150-foot parabolic antenna. Reception in the spacecraft will be by means of coaxial whip antennas and phase-locked receivers. Digital output circuitry is designed to make Doppler, group path, and amplitude measurements and encode these onto the tele-

metry channel for transmission to the NASA deep-space tracking site at Goldstone, California.

Figure 4 is a sketch of the spacecraft. The antenna for the propagation experiment is shown at the lower right. Figure 5 shows the trajectories of the two spacecraft in the ecliptic plane relative to the earth-sun line.

The design lifetime of the deep space probes based on the maximum communication range is about 200 days, and the maximum range from the earth to the two probes would be 0.5 AU to 0.7 AU. Pioneer A would go to about 0.8 AU from the sun, while Pioneer B would go out to about 1.2 AU.

For the chosen two frequencies, $n = 8.5$ so that $(n^2 - 1)/n^2$ is nearly unity. Thus we can use 50 Mc as the frequency in (3) and (4) to determine measurement capabilities. From (4), one cycle change between 50 Mc and the appropriate subharmonic of 425 Mc corresponds to a change in I of about 4×10^{14} electrons/m^2. To detect the sense of the change, a bias of 5 cps will be used so that there would be 300 beats during one minute between 50 Mc and the 425 Mc subharmonic when the medium is not changing. The count would be 301 if the integrated interplanetary density increased by 4×10^{14} m^{-2}, and 299 if it decreased a similar amount. At a range of 0.5 AU, this change in the integrated electron density would correspond to an average volume density change of about 5000 m^{-3}, or only 0.005 electrons/cm^3.

Both frequencies will be sine-wave modulated in phase at the transmitter. The modulation phase difference will be determined at the spacecraft for the group delay measurement. Either one of two modulation frequencies, 8.7 and 7.7 kc, will be used. From (3) it can be shown that the total electron content I can be measured to about $\pm 4 \times 10^{16}$ m^{-2}, or an average volume density at 0.5 AU of 0.5 cm^{-3}, assuming that the modulation phase is measured

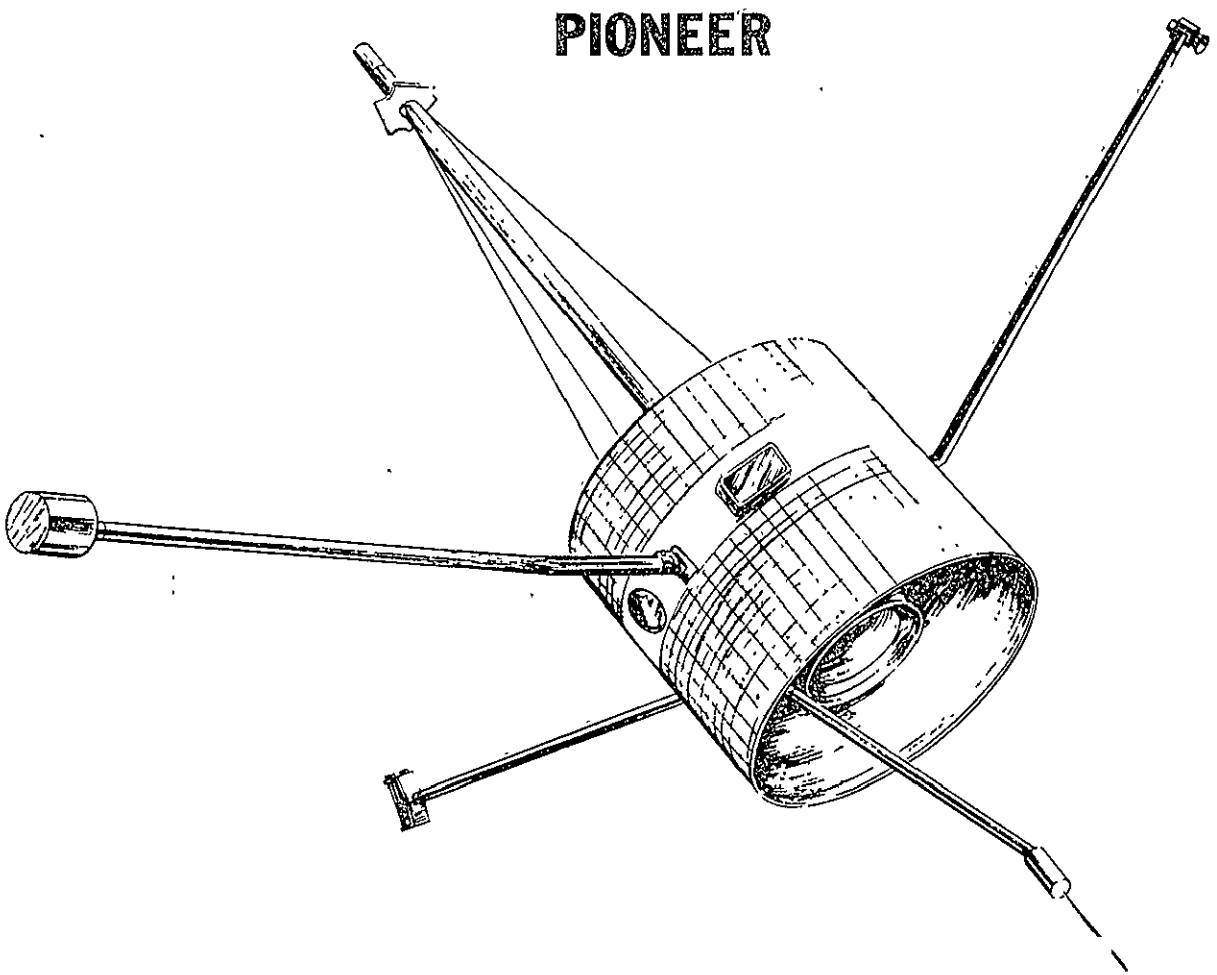

Fig. 4 THE PIONEER INTERPLANETARY SPACECRAFT SCHEDULED FOR FLIGHT IN 1965

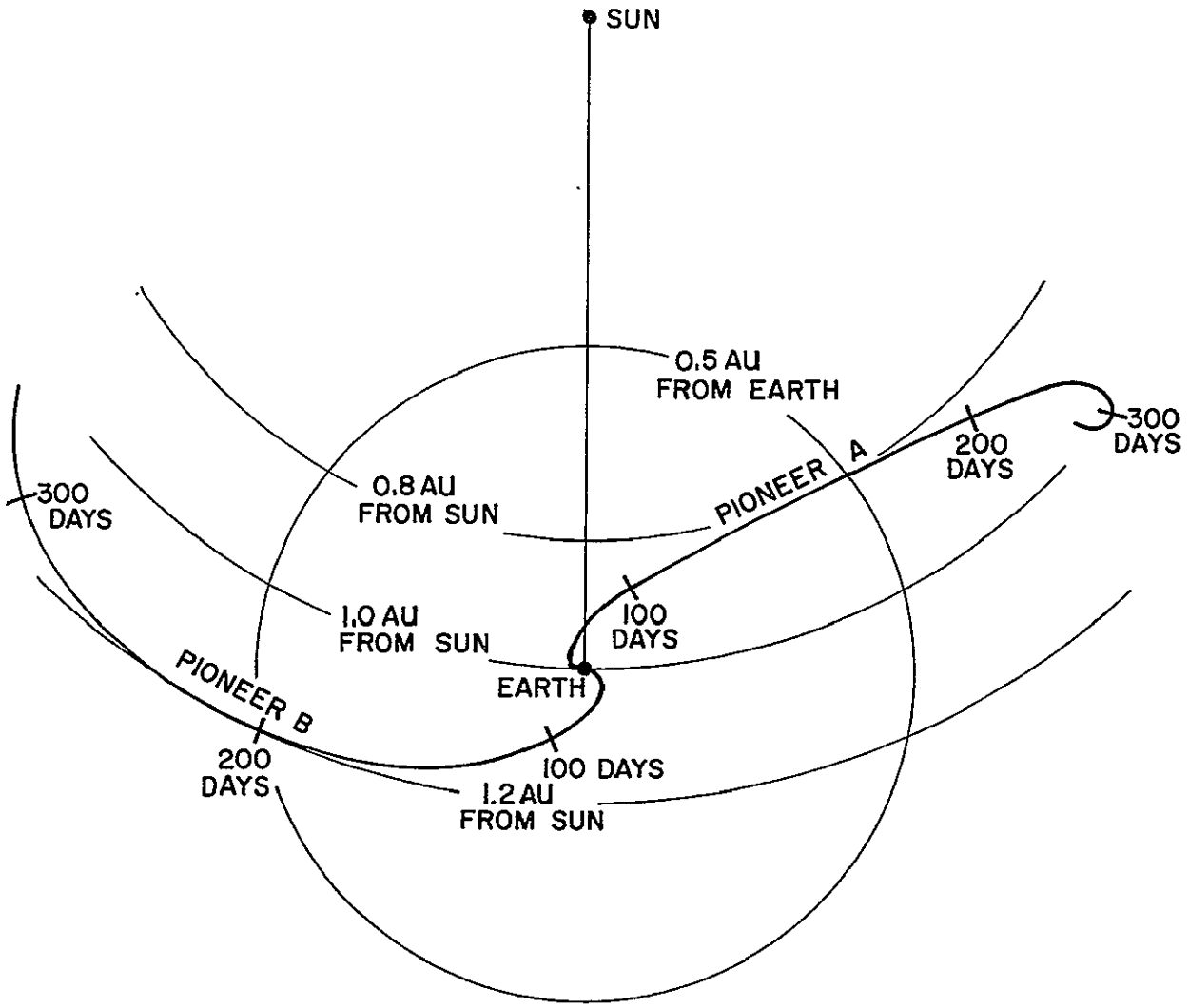

Fig. 5 NOMINAL TRAJECTORIES FOR THE INTERPLANETARY SPACECRAFT PIONEER A AND B

to ± 6°. By having two modulating frequencies, any possible ambiguity due to more than one cycle of modulation phase difference can be evaluated.

Because of the great range to the spacecraft, the value and time changes of I in the ionosphere and magnetosphere will not add much uncertainty in the measurements of the interplanetary medium. It is estimated that these uncertainties due to near-earth ionization will be about the same as the measurement accuracies given above.

Measurements of amplitude are included for several additional experiments. It has been proposed that the spacecraft be fired on a trajectory such that they will be occulted by the moon, as seen from the earth, one or more times during their flight. If there is a lunar ionosphere having a volume density as low as 100 cm^{-3}, it will bend the tangential 50 Mc rays more than the 425 Mc rays, and this would show up at the spacecraft as a difference in time of signal extinction at the two frequencies. This subject is discussed in greater detail in the next section.

It has been suggested by Lusignan[10] that the relativistic increase in mass of streaming electrons in the solar wind should cause a polarization effect on radio waves propagating through the interplanetary medium. At the spacecraft, polarization changes of the incident wave will be detected as characteristic amplitude changes due to the fact that the antenna and spacecraft will be spinning.

With two probes in space at the same time, it should be possible to monitor how a solar stream progressively fills the two propagation paths. Plasma instruments and magnetometers on the spacecraft, and studies near the earth, could give more detailed but more localized information about the stream. Such complementary studies should provide important new information about the density, dynamics, and other characteristics of the interplanetary medium.

5. PLANETARY IONOSPHERES AND ATMOSPHERES[11]

a. Ionospheres

Radar probing of planetary ionospheres is possible in principle by monostatic earth-based radar, monostatic probe-based radar (topside sounding), or bistatic radar. In bistatic radar, the surface of the planet might be used to return a signal which penetrates the ionosphere in order to make Doppler, group path, etc., measurements of ionospheric effects, or a variable low frequency might be used which would be reflected at various levels in the ionosphere itself.

Another bistatic possibility which appears much easier to implement than any of the above (assuming the advent of the space age) requires occultation of a spacecraft by the planet as seen from the earth. Radio waves propagating between the earth and the spacecraft would then pass tangentially through the ionosphere and atmosphere.

Monostatic radar from the earth would be troubled by the earth's ionosphere, and extremely large transmitter powers at relatively low frequencies would be required, as described previously. Similar trouble would be encountered in the bistatic mode involving reflections from the planetary ionosphere. Spacecraft instrumentation for topside sounding and for using surface-reflected signals would be considerably more complex than is required for the bistatic occultation method.

Figure 6 illustrates the geometry of the occultation problem. It is obvious that such occultation measurements could be accomplished either with a fly-by or an orbiting trajectory. Assuming spherical symmetry of the plasma around the planet, a trajectory that lies outside the sensible ionosphere and magnetosphere, and straight-line propagation between the earth and spacecraft, the integrated electron density as a function of closest approach

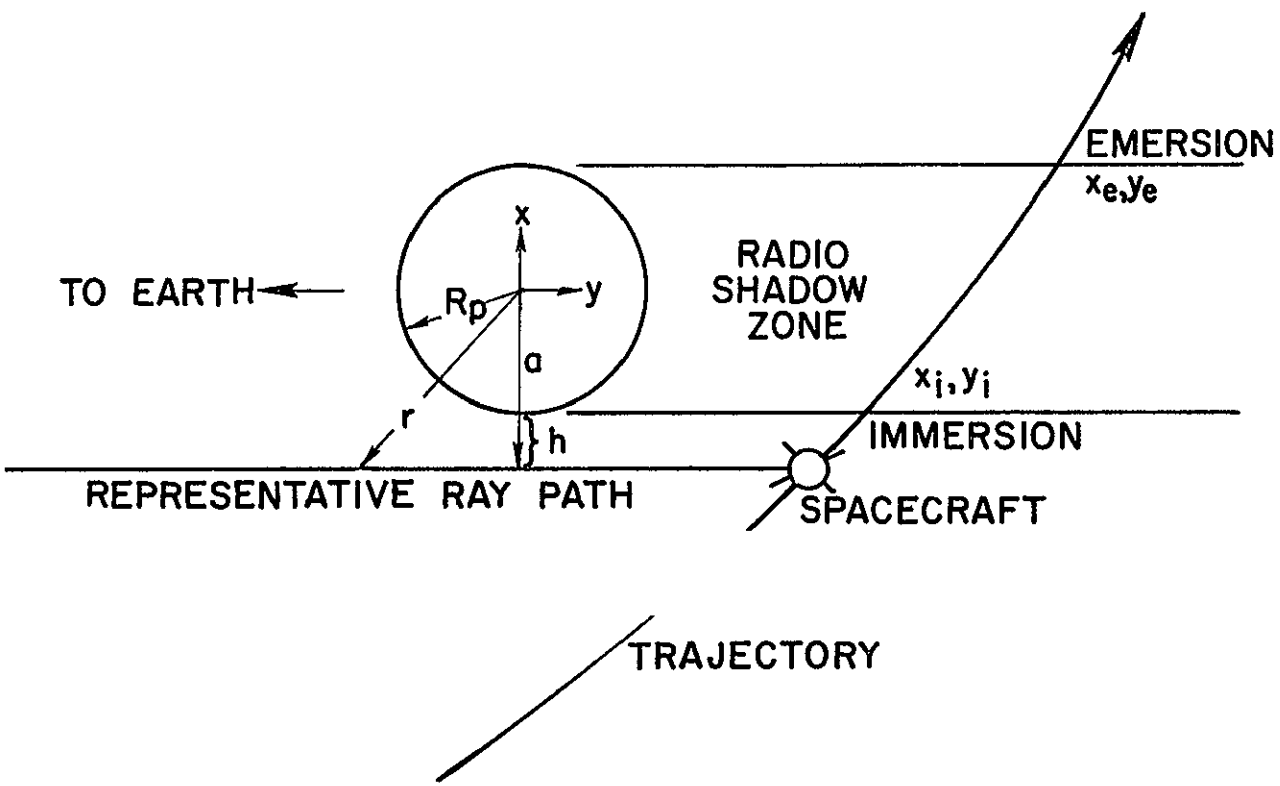

Fig. 6 SIMPLIFIED GEOMETRY OF PLANETARY OCCULTATION OF A FLY-BY OR ORBITING SPACE PROBE

of the ray to the planet's center (a) is given by

$$I(a) = 2\int_{0}^{\infty} \frac{N_e(r)rdr}{(r^2 - a^2)^{\frac{1}{2}}} \qquad (13)$$

In practice, I(a) would be found from I(t) measurements by making use of the measured spacecraft position as a function of time. If a measurable amount of the neutral atmosphere is intercepted, (13) could be adjusted to include its effects as indicated in (10) and (11). The problem is also tractable for a non-spherically symmetric ionosphere if the law of the departure from symmetry is known, such as would be the case for a theoretical electron volume density dependence on solar zenith angle. The correction for lack of symmetry is expected to be relatively unimportant, however[12].

The function I(a) in (13) can be measured directly from group delay (3), by integrating the Doppler excess (4), or doubly integrating gain measurements (8). If the magnetic field strength and orientation is known, Faraday polarization measurements (5) could also be used. On the other hand, polarization measurements might first be used to estimate the near-planet magnetic field strength using knowledge of the plasma density gained in the other measurements. Absorption measurements (6) and ray bending (7) could also be measured for additional information and as a check on the other determinations.

Once I(a) is determined, (13) can be inverted to solve for the volume density profile of the electrons, $N_e(r)$, or the profile of refractivity N(r). This problem corresponds to the solution of Abel's integral equation which has been used extensively in ionospheric physics to determine the true-height electron density profile from vertical ionosonde records[13].

Corrections will probably be required in practice for

higher-order effects (e. g., ray bending affects phase path) than given in the above simplified formulas. This can be accomplished either by the use of analytical expressions that include higher-order terms, or by an iterative process involving the determination of a first-order profile for which correction terms can be computed, etc.[12].

From a consideration of the possible ionospheric measurement methods from the viewpoint of accuracy and ease of implementation, it appears that a Doppler excess measurement based on the use of two harmonic frequencies would be preferred. This would give $I_t(a)$ from which $I(a)$ would be found by integration. Group path, amplitude, polarization, etc., measurements could be added as may be feasible for extension and check of the Doppler measurements.

Consider, for example, the ionosphere and atmosphere of Mars. By way of illustration we will assume a Chapman ionosphere with its maximum density at a height above the surface of 320 km, and a scale height of 130 km. Chamberlain's[14] model of the ionosphere of Mars has a daytime maximum volume density of 10^{11} m^{-3} and this value is used in this example. For the neutral atmosphere, we assume an exponential profile of scale height 16 km with a surface pressure of 25 mb, corresponding to the studies of Kaplan, Munch, and Spinrad[15]. The temperature of the atmosphere is assumed to be 250° K.

Figure 7 shows the refractivity profile N(h) for this assumed atmosphere and ionosphere. Figure 7(a) is for a frequency of 50 Mc while 7(b) is for 400 and 2300 Mc. Note the great change in the scale for N in (a) as compared with (b). The refractivity of course varies as f^{-2} for the ionosphere, but is independent of frequency for the neutral atmosphere. (For the atmosphere it was assumed that the average α_n in (9) is the same as for the earth's dry atmosphere, and this would be approximately true for the ex-

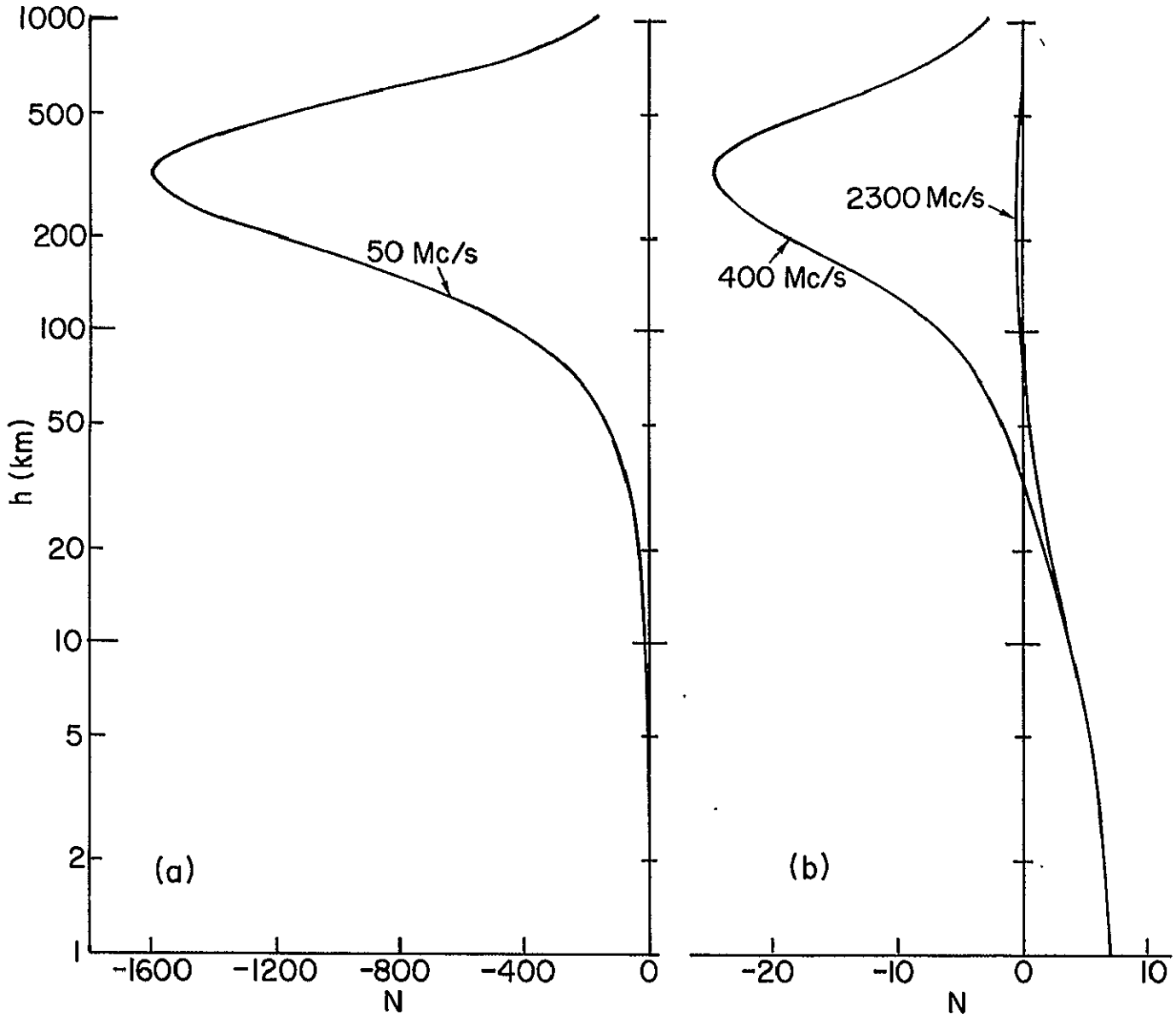

Fig. 7 REFRACTIVITY PROFILE IN HEIGHT OF ASSUMED MARTIAN IONOSPHERE (PEAK DENSITY 10^{11} m^{-3}) AND ATMOSPHERE (SURFACE PRESSURE 25 mb) AT 50, 400, AND 2300 Mc (SEE TEXT).

pected constituents in the atmosphere of Mars.)

As expected from (12), the ionospheric effect at 50 Mc (- 1600 N units maximum) is very large compared to that at 400 Mc (- 25 N units maximum) so that one could consider that the 400 Mc signal acts as an unperturbed reference for automatic cancellation of the Doppler effect due to path length change, and for avoiding the necessity of making very precise measurements of frequency. With regard to this model, the effect of the neutral atmosphere (+ 7 N units maximum) is so small that it can be neglected as compared to the ionospheric effect at the lowest frequency.

Figure 8 shows the asymptotes of the ray paths for 50 Mc near Mars. The angles of refraction are very small (the maximum here is about 0.5°) so that a greatly compressed horizontal scale is used in the figure. For trajectories beyond about 50,000 km behind the planet, the spacecraft is in areas where the ray paths cross over and form caustics, so that the measurements could not be simply interpreted as discussed above. For close-in trajectories, however, the spacecraft is always within the region where no confusion can arise due to the formation of caustics. From 8, the distance y_c to the cross-over point of adjacent rays is

$$y_c = \left(\frac{2\pi}{c^2 r_e}\right) \frac{f^2}{I_{xx}} \qquad (14)$$

Figure 9 shows the 50 Mc phase advance (to be obtained in practice by integrating I_t) and the values of I(a) for this model ionosphere, plotted as a function of $h = a - R_p$, the distance by which an earth-probe straight line would miss the planetary surface. The solid curve would result from using the simple formulas given above, while the dashed curve for phase advance includes the correction due to ray bending[12].

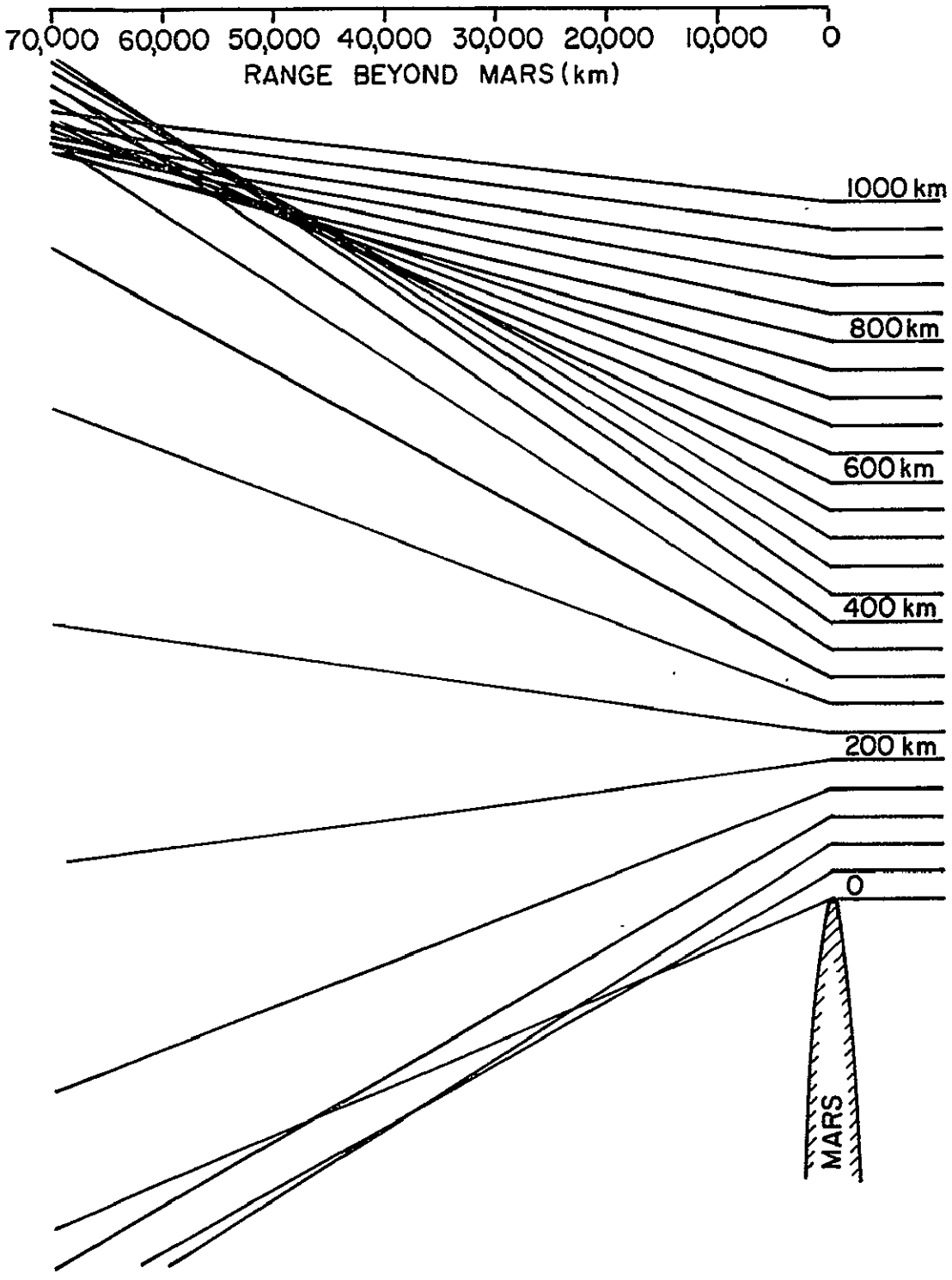

Fig. 8 ASYMPTOTES OF 50 Mc RAY PATHS NEAR MARS FOR THE ASSUMED IONOSPHERE

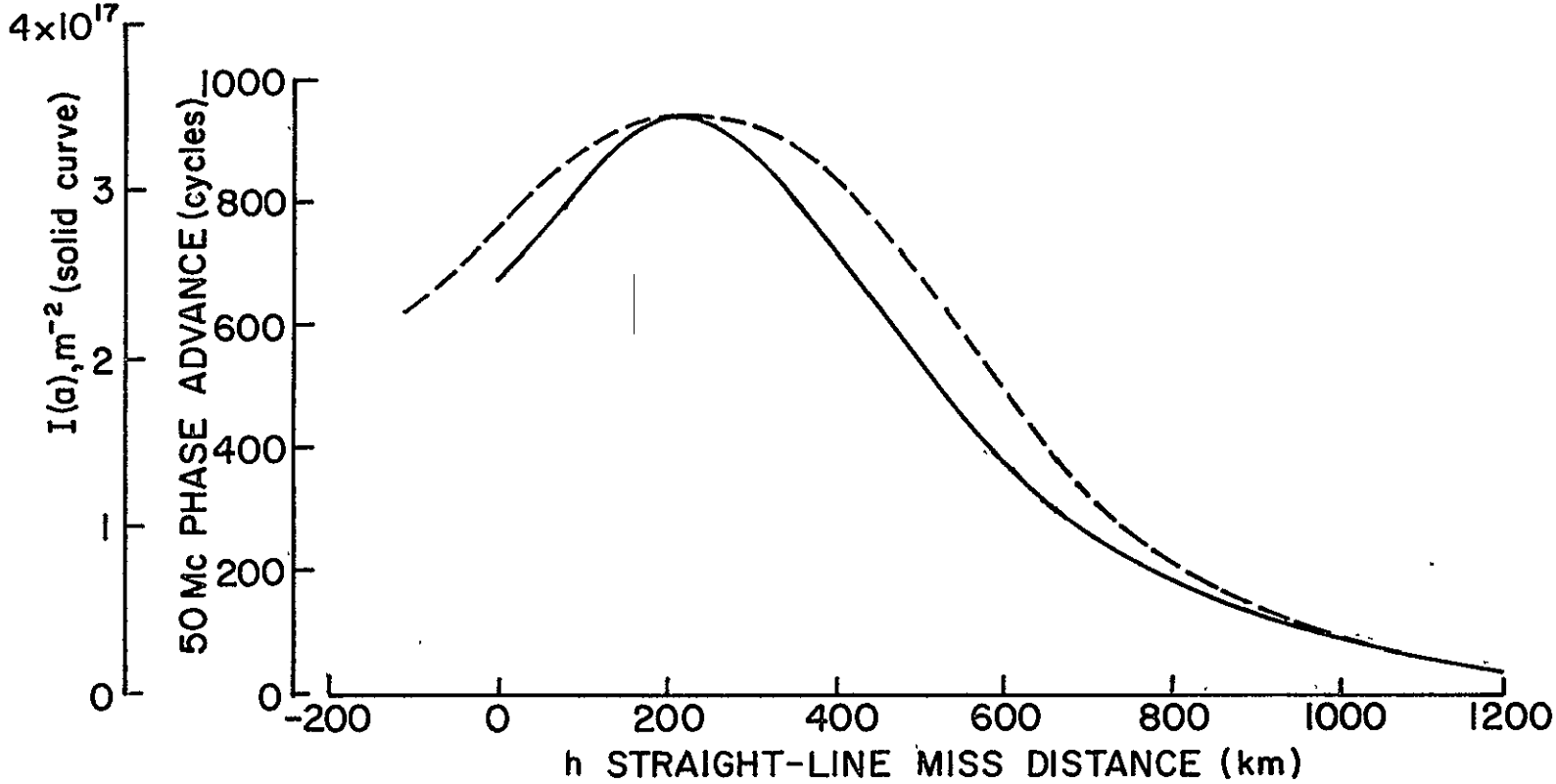

Fig. 9 PHASE ADVANCE AT 50 Mc AND INTEGRATED ELECTRON DENSITY FOR THE ASSUMED MARTIAN IONOSPHERE. THE SOLID CURVE REPRESENTS BOTH QUANTITIES TO FIRST ORDER. THE DASHED CURVE FOR PHASE ADVANCE INCLUDES THE CORRECTION DUE TO RAY BENDING. IT IS ASSUMED THAT THE SPACECRAFT IS 15,000 km BEHIND MARS.

Figure 10 shows the 50 Mc signal gain due to ionospheric focussing plotted as a function of h. This was computed from the more exact first expression for G in (8). Since immersion and emersion of the spacecraft would occur at different known values of y (except for a spacecraft in a circular orbit), it should be possible to separate y-dependent focussing gain (8) from absorption (6) which would be independent of the distance to the spacecraft.

For a fly-by trajectory, dx/dt would be on the order of one or two kilometers per second, so that the occultation measurements over a height range of about 1000 kilometers would be made in less than about fifteen minutes. Measurement accuracy in this example would correspond to one part in a thousand at the maximum value of I if the Doppler excess is counted to an accuracy of one cycle. Changes in the earth's ionosphere and in the interplanetary medium would set the limiting accuracy due to the environment. It does not appear that such uncertainties could have an appreciable effect unless there were very unusual and large scale changes in the interplanetary medium during this short measurement period.

b. Atmospheres

As seen from the above example, relatively low radio frequencies are desirable for ionospheric measurements. Because of the very large transmitter power requirements at low frequencies, it appears important that the transmitters be on the earth and the receivers on the spacecraft. Nevertheless, the first ionospheric measurements may actually be made using spacecraft transmissions, as a byproduct of the currently-planned atmospheric measurements of Mars.

A major engineering constraint to the exploration of the Martian surface is the uncertainty in the atmospheric parameters which affect entry and soft-landing of a probe on the planet. Estimates of surface pressure which have

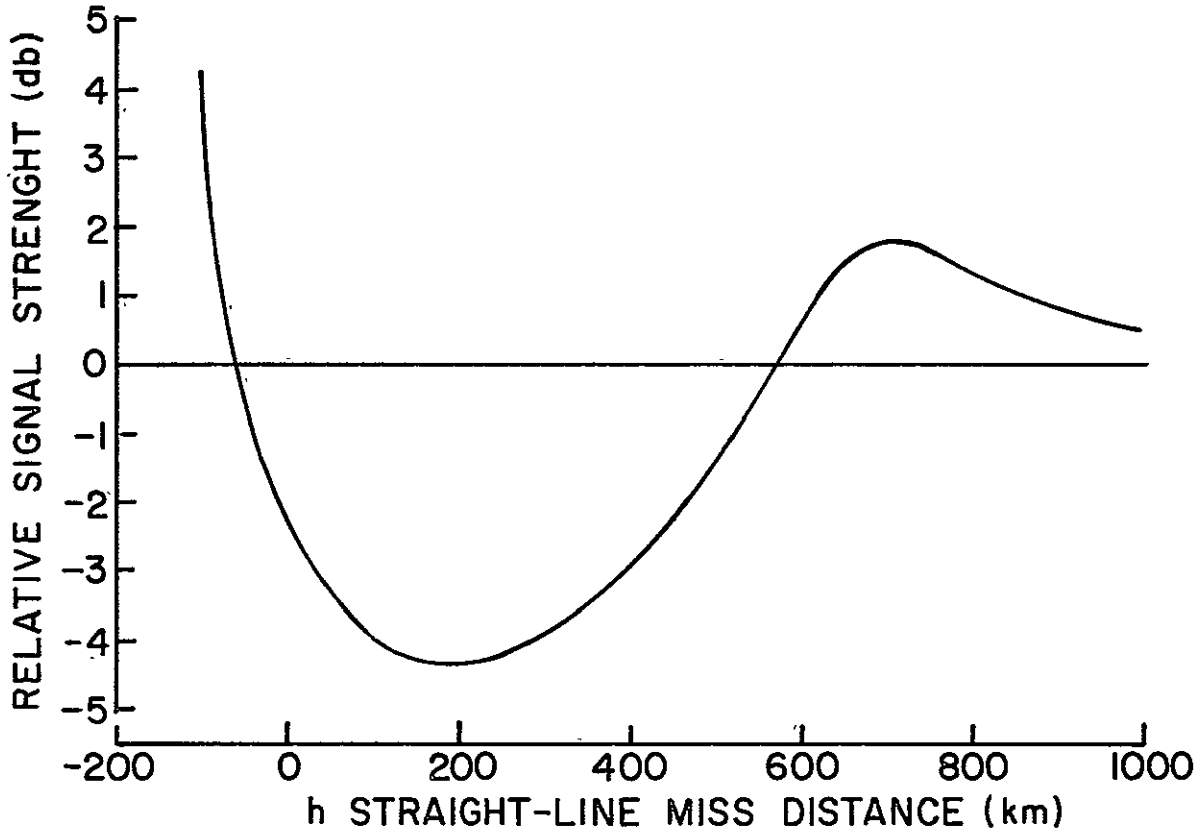

Fig. 10 FOCUSSING GAIN AT 50 Mc IN THE ASSUMED IONOSPHERE FOR A SPACECRAFT 15,000 km BEHIND MARS

been made range from less than 10 mb to more than 100 mb. A group (A. J. Kliore, F. D. Drake, D. L. Cain, and G. S. Levy) from the Jet Propulsion Laboratories together with G. Fjeldbo and the author from Stanford have proposed that the occultation of the S-band telemetry signals on the Mariner spacecraft, which will be sent to Mars in 1964 and 1966, be used to make atmospheric measurements.

From Figure 7(b) it is seen that an atmosphere of 25 mb surface pressure has a very slight refractive effect compared with the effect of the ionosphere at 50 Mc. The 2300 Mc telemetry signal, on the other hand, is sufficiently high that with the above atmosphere-ionosphere model, the atmospheric perturbations would be predominant.

Since atmospheric refractivity is non-dispersive, absolute frequency and amplitude measurements must, in general, be made. That is, the convenient self-calibration characteristics of dual-frequency ionospheric measurements are not applicable here. By use of a transponder technique, a ground-based frequency standard can be used so that extremely small (one part in 10^{11}) effects can be measured.

The occultation measurement of the atmosphere is in several respects an ideal experiment. It requires no added weight, power, space, or information capacity in the spacecraft, since use is made of the existing telemetry signal.

The profile of atmospheric refractivity depends upon pressure, temperature, and constituent profiles. Except for a small uncertainty about the effects of unknown constituents, however, refractivity is most closely related to p/T or density, so that it is a good measure of the probe-entry characteristics of the atmosphere. There are several different frequency and amplitude measurements that give independent information on p/T and T/$\bar{m}$ ($\bar{m}$ is the average molecular mass) at the surface, so that some separation of parameters is possible. Combining this with other

information on temperature and probable constituents makes it possible to use the radio information to help determine actual constituents, pressure, temperature, and density.

The JPL group plans to make frequency measurements, but in order to find f_{DE} in (4) it will be necessary to know the Doppler due to changing spacecraft motion to an accuracy of about one part in 10^5. Nevertheless, they estimate that the surface pressure can be determined to an accuracy of better than 5% if the pressure is near 25 mb, and better than 10% if it is near 10 mb.

The Stanford group plans to use the amplitude measurements to find atmospheric defocussing (8), and, in addition, to study the effects of the atmosphere on the Fresnel diffraction pattern produced at the limb of Mars. Figure 11 illustrates the difference between vacuum and atmospheric occultation at 80,000 km behind Mars, assuming a frequency of 2300 Mc and a 100 mb surface pressure. The extension of the period of the Fresnel fluctuations (Fresnel "stretch") appears to provide a very sensitive measure of near-surface atmospheric conditions. In addition, the gain (- 8 db in this example) and the time-rate-of-change of gain give independent information on surface density and scale height. Finally, this figure also illustrates that there is a difference in time of occultation for vacuum and atmospheric conditions, and this would provide another atmospheric measure if the diameter of Mars is known to a few kilometers. It appears more likely, however, that this last measurement plus other atmospheric measurements would serve instead to improve our information on the diameter of Mars.

For an exponential atmosphere, it can be shown from (11) and the earlier equations that the maximum first-order atmospheric effects depend upon surface refractivity N_o, scale height H, and planet-probe distance y as:

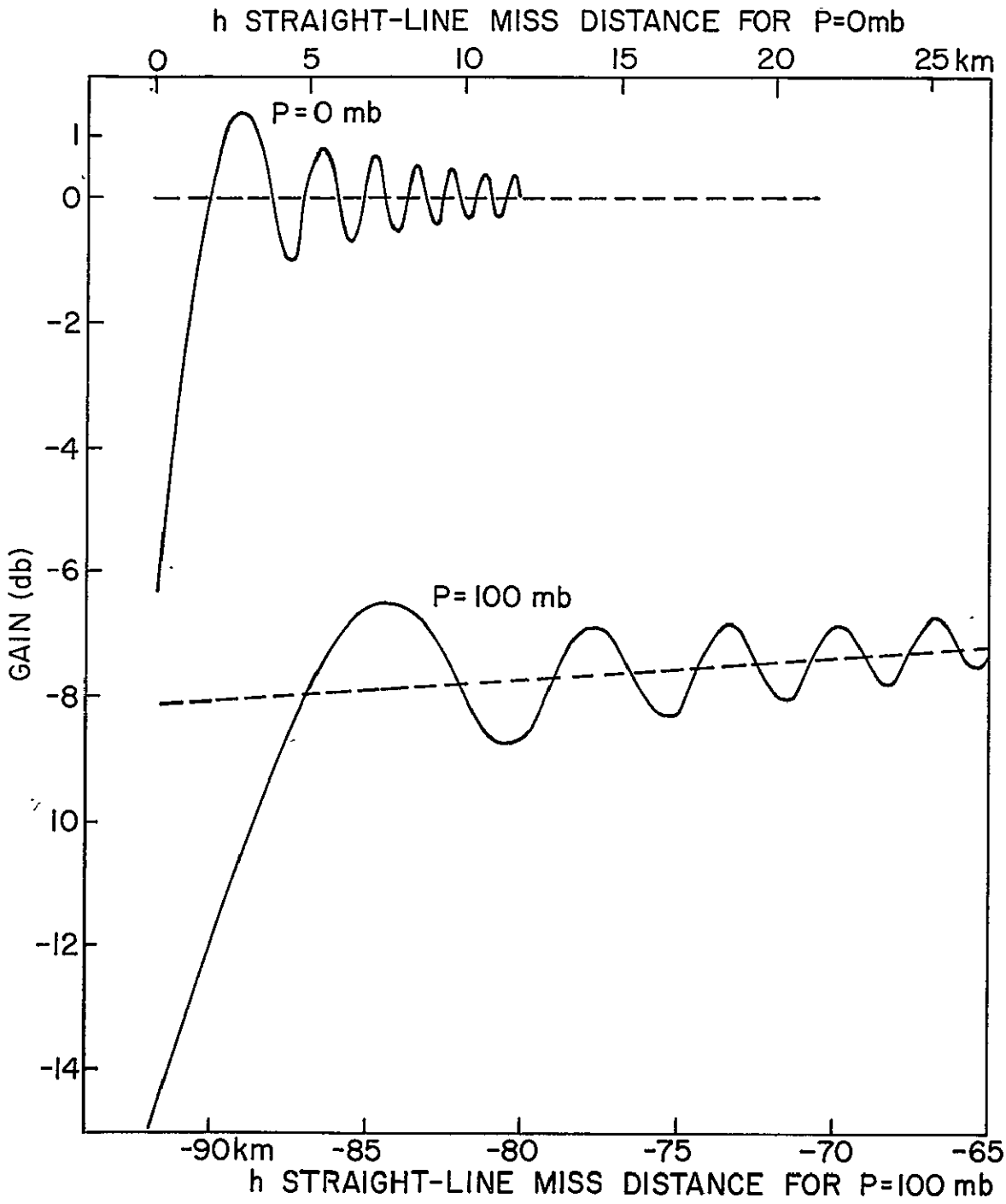

Fig. 11 FRESNEL PATTERNS DUE TO LIMB DIFFRACTION WITH AND WITHOUT AN ATMOSPHERE OF SURFACE PRESSURE EQUAL TO 100 mb, A SCALE HEIGHT OF 16 km, AND A TEMPERATURE OF 250 °K. It is assumed that the spacecraft is 80,000 km behind Mars. Note that the two curves have different abscissas, top and bottom.

focussing gain and Fresnel stretch	$\sim N_o y H^{-3/2}$
time or space rate of change of focussing gain	$\sim N_o y H^{-5/2}$
phase	$\sim N_o H^{1/2}$
frequency	$\sim N_o H^{-1/2}$
time or space delay to signal extinction	$\sim N_o y H^{-1/2}$

(15)

Figures (12) and (13) give computed examples of the profile of frequency and gain as the spacecraft is immersed or emerges at 20,000 km behind the planet for 25 and 100 mb surface pressures, assuming H = 16 km, T = 250° K, and f = 2300 Mc. The maximum Fresnel stretch would be 16% and 56% for the two pressures in this example.

Surface roughness at the limb of the planet is expected to wash out high-order Fresnel fluctuations, but from radio-astronomical measurements of the occultation of radio stars by the moon, it is not expected that rough planetary limbs will seriously degrade an atmospheric measurement based on diffraction.

The principal uncertainty in the 2300-Mc occultation experiment on Mars appears to be the possible effect of a dense ionosphere. In the example given above, it was shown that a Chapman layer with a maximum electron density of 10^{11} m^{-3} had much less of an effect at this frequency than did the atmosphere. However, the ionospheric model from Chamberlain[14] was based on a surface pressure of 85 mb (2 mb CO_2 and 83 mb N_2), while recent studies[15] indicate a much lower pressure of 25 ± 10 mb, with 3 to 6 mb of CO_2 and either N_2 or A as the principal remaining constituent. Because of the greater amount of CO_2 to provide the principal ion O^+, and a lesser amount of N_2 to act through ion-

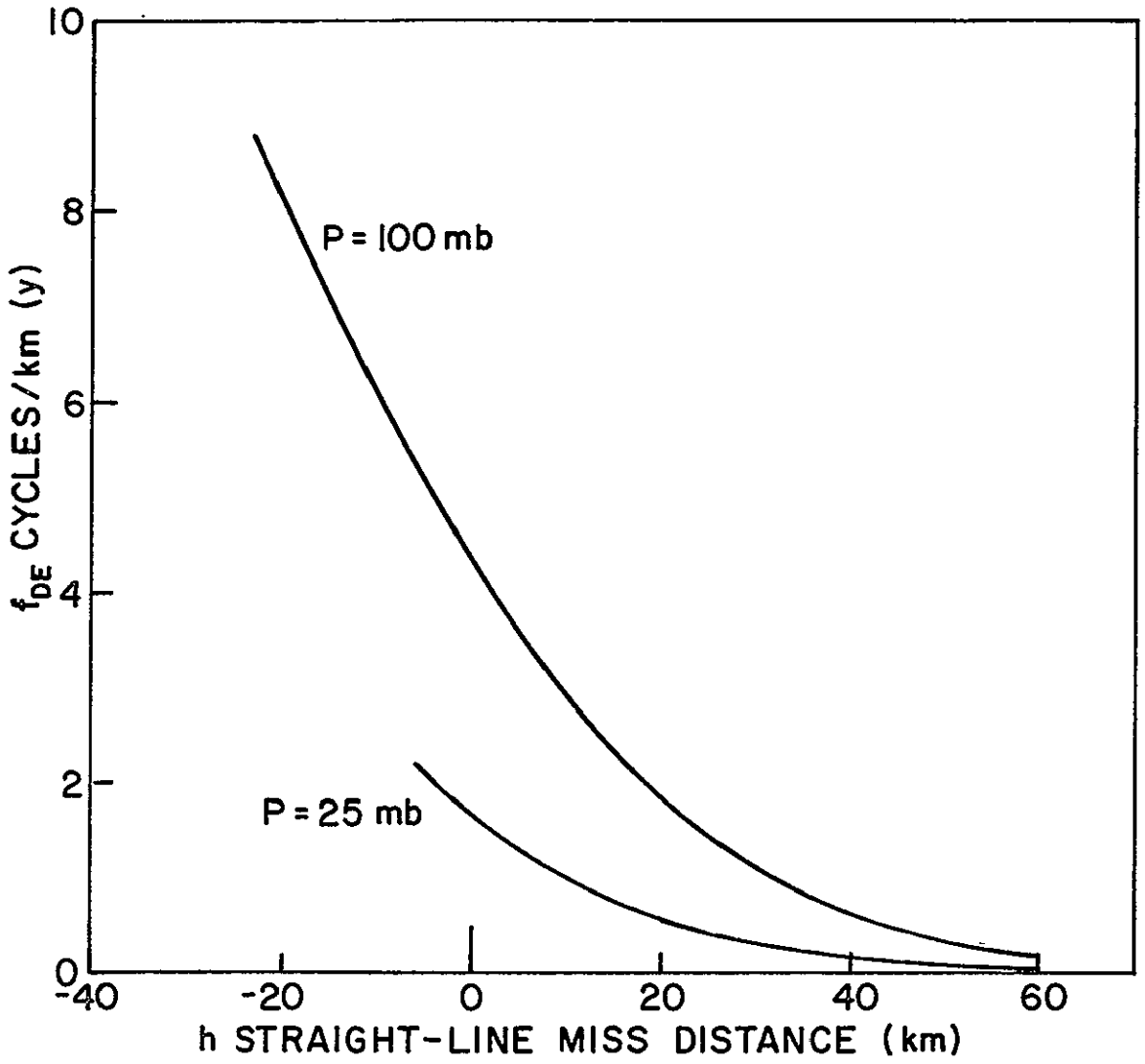

Fig. 12 CHANGES WITH TIME OF THE DOPPLER EXCESS FREQUENCY AT 2300 Mc DUE TO THE ATMOSPHERE FOR TWO VALUES OF SURFACE PRESSURE AND A PROBE - MARS DISTANCE OF 20,000 km

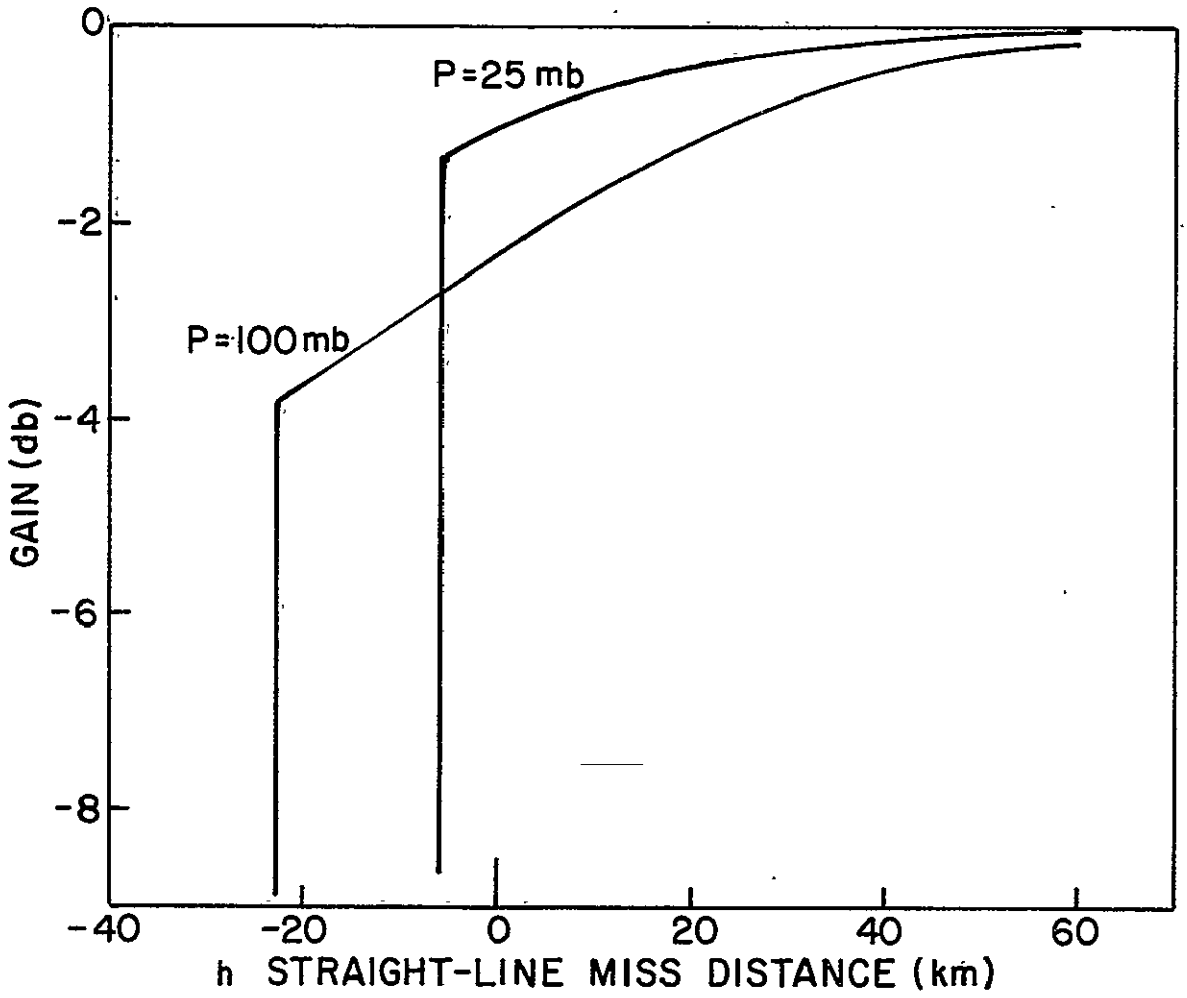

Fig. 13 CHANGES WITH TIME OF THE AVERAGE SIGNAL STRENGTH DUE TO ATMSOPHERIC FOCUSSING FOR TWO VALUES OF SURFACE PRESSURE AND A PROBE - MARS DISTANCE OF 20,000 km

atom interchange and dissociative recombination to provide an electron loss mechanism, the new low-pressure atmosphere could have an ionosphere of markedly greater density than in the Chamberlain model. If this increase is not too great, the S-band experiment could provide both an electron density ionospheric profile and a neutral density atmospheric profile. On the other hand, a very high ionospheric density or sharp density gradients could mask the atmospheric effect. In general, it would be advantageous to use several frequencies simultaneously in such an occultation experiment so that dispersive and non-dispersive refraction could be experimentally separated.

6. SOLAR RADAR ASTRONOMY

Monostatic radar echoes from the sun have been obtained at 26 Mc and at 38 Mc. Bistatic methods similar to those discussed in sections 4 and 5 can be used to study the inner and outer solar corona when space probes become available which can be sent behind the sun.

Marginal returns were obtained at Stanford in April 1959[16] and again in September 1959[17] at the lower frequency, using four or eight rhombic antennas (covering 14 or 28 acres) and a CW transmitter power of about 40 kw. Antenna gains are estimated at 25 to 28 db. Coding and computer data processing techniques were used to demonstrate that there was a return (at a S/N ratio of about - 23 db before integration) corresponding to reflection at about 1.7 solar radii, that the Doppler frequency spectrum of the echo must be wider than the 2 kc/s receiver bandwidth, and that the echo strength in this bandwidth corresponded to a radar cross section approximately equal to one to two times the photospheric disc size. Data from 16 minute runs made on several different days had to be combined to produce sufficient signal-to-noise ratio to demonstrate the

presence of an echo. Figures 14(a), (b), (c) illustrate the echo indications at 26 Mc, and Figure 14(d) is a corresponding illustration from early results with the 38 Mc system discussed below.

At 38 Mc, routine radar studies of the sun have been made since April, 1961, by the MIT Lincoln Laboratory at a site near El Campo, Texas[18,19,20]. Transmitter power is up to 500 kw CW, and the antenna now consists of two crossed-polarized arrays of dipoles, one with a measured gain of 33 db and the other 36 db. One 16-minute coded transmission is sent per day, the azimuthal beamwidth being sufficient for only one transmit and receive period. The higher gain antenna is used for transmission and both are used for reception. Measured Doppler spread of the echo varies between 20 and 70 kc, with the center of the spectrum shifted up in frequency by an average of about 4 kc. This upward shift represents a net outward flow of plasma at the reflecting level.

Radar cross sections vary from a high of about 16 times the photospheric disc size down to a level that is undetectable by this system. Average values correspond approximately to the size of the photosphere. The energy appears to be returning from a level in the corona corresponding to about 1.5 solar radii, and the spectral and range-spread evidence indicates that this level is rough and rapidly moving[20] with both random and directed velocities. Figure 15 consists of range-Doppler spectra for four relatively strong echoes, and these illustrate the wide band-width and range spread. There is a decided net positive Doppler shift with the range intervals nearer the earth showing the largest effects. This has been interpreted[19,20] as evidence of the solar wind near its source.

From the 38 Mc results[20] it appears that the echo energy in the Stanford experiment should have been spread

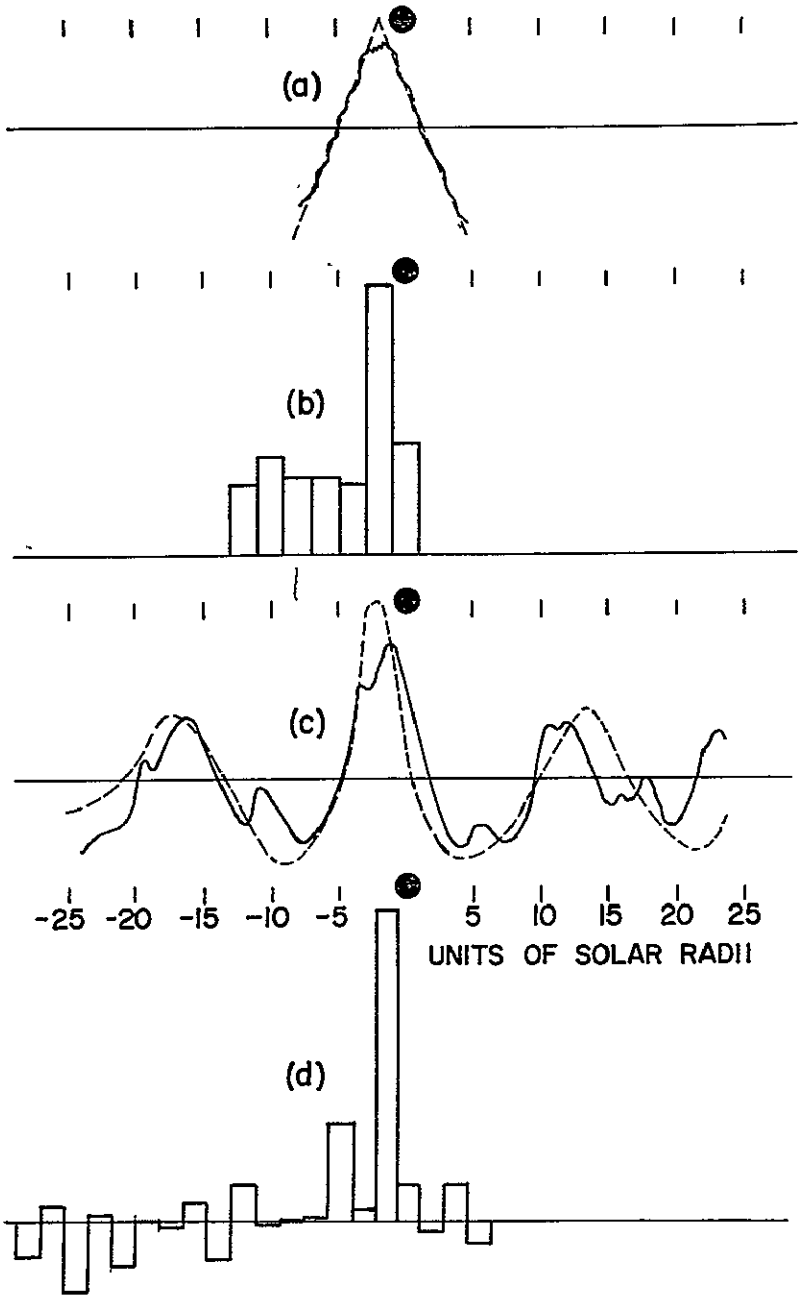

Fig. 14 In (a) the solid curve is the cross correlation of the solar echo data taken at Stanford in April, 1959, and the dashed line is the ideal correlation corresponding to reflection at 1.7 solar radii[16]. In (b) the same data are analyzed in terms of the positions of significant peaks in the integrated return, and the largest number of such peaks are at a range position corresponding to solar reflection. Curve (c) shows the ideal (dashed) and measured (solid) correlation for the more complicated code used in the September, 1959, tests, the central peak corresponding to the range of the echo[17]. In (d) echo energy is plotted as a function of range for the early 38 Mc measurements at El Campo, Texas, the result being the sum for a number of days in the period April to July, 1961[18]. In each graph the circle represents the size of the photospheric disc relative to the range scale.

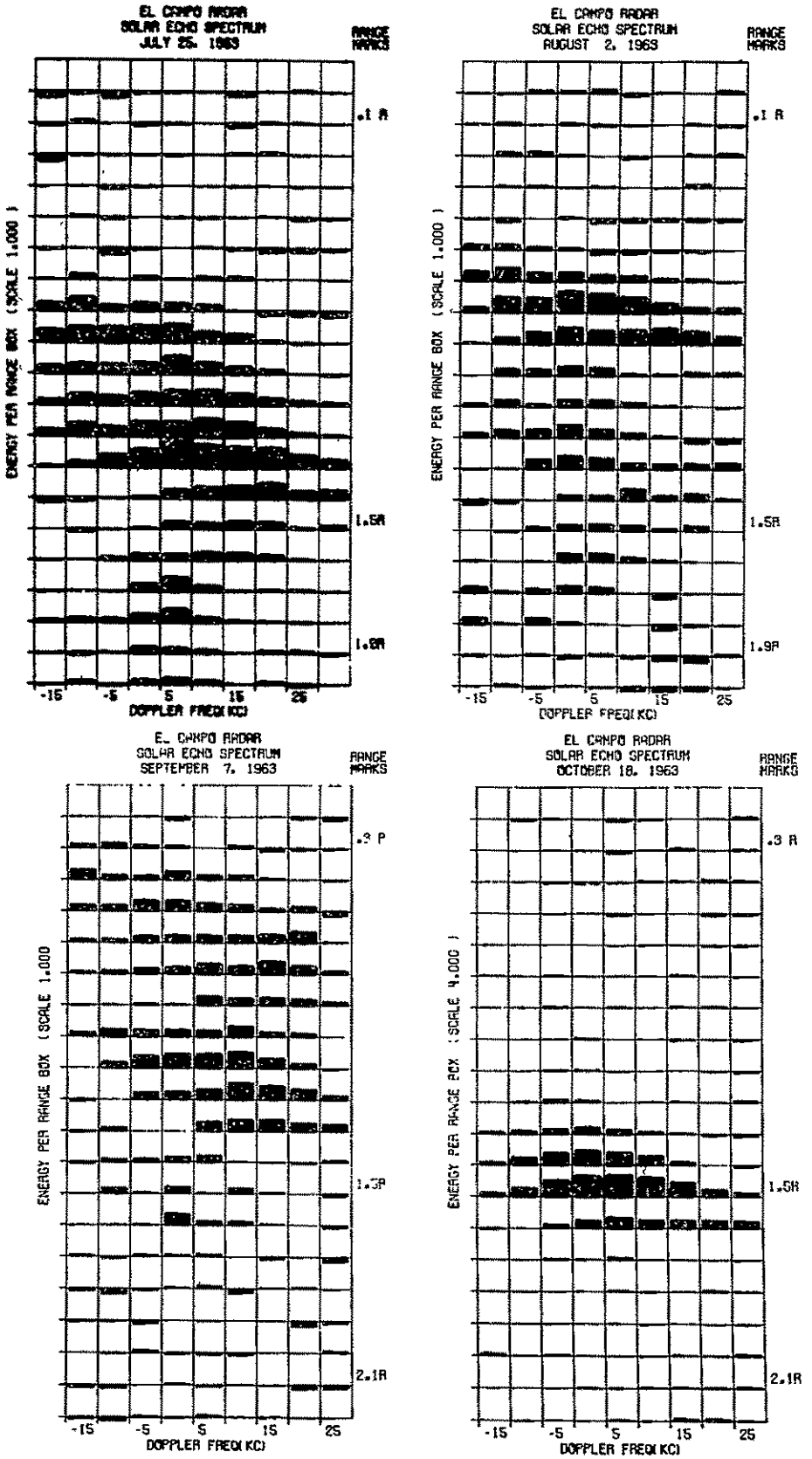

Fig. 15 RANGE - DOPPLER SPECTRA OF FOUR SOLAR RADAR ECHOES OBTAINED AT THE LINCOLN LABORATORY FIELD SITE NEAR EL CAMPO, TEXAS (courtesy of J. James, Lincoln Laboratory). The vertical range scale corresponds to reflection at the indicated number of solar radii, in units of 0.1R, and the horizontal scale is doppler frequency intervals in units of 5 kc.

from 6 to 25 times as wide as the receiver bandwidth of 2 kc. Thus the solar radar cross section at the lower frequency would be perhaps an average of 10 times the measured value. This would make it considerably higher than the average radar cross section measured at 38 Mc, but still within the measured range of fluctuation of these results. Two factors are expected to contribute to this difference.

Figure 16 shows computed values by Yoh[21] of the expected solar radar cross section as a function of wavelength, assuming spherical symmetry and various electron temperatures and densities. (The n values are multiplicative factors to be used with the Allen-Baumbach[22] model of the solar corona.) These curves include the effects of ray bending and absorption in this model corona. (The simple formulas given above are not applicable to this problem since complete reflection and high absorption may be encountered.) Note in particular that over the plotted wavelength range, the solar radar cross section increases with wavelength. For a relatively low electron density of a half million degrees, the 26 Mc results might be expected to give a radar cross section as great as ten times the 38 Mc value, due primarily to less absorption above the reflecting level. The theoretical absolute values of radar cross sections under these conditions are less than the measured values, but this could result from the increased cross section of the actual rough target over the theoretical smooth model. The possibility that the electron temperature may be lower than previously suspected is supported by the radar measurements of turbulence in the corona. That is, some of the relatively high estimates of temperature are based on Doppler broadening of coronal emission lines assumed to be due to thermal motion of the electrons. If the electrons have large mass motions in addition to their thermal motions, then over-estimates of electron temperatures would be made by this method[20,23].

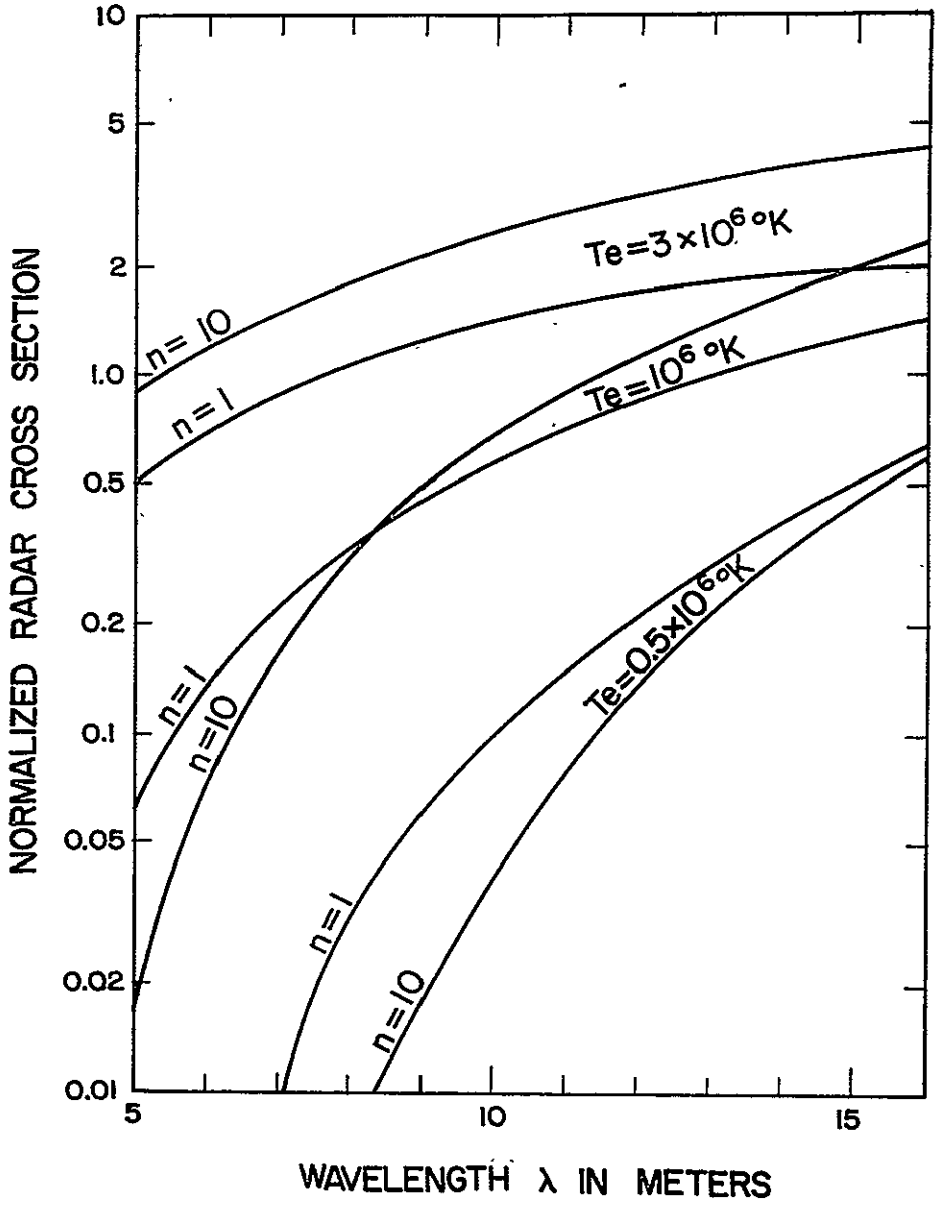

Fig. 16 THEORETICAL RADAR CROSS SECTION OF THE SUN, NORMALIZED BY THE AREA OF THE PHOTOSPHERIC DISC, PLOTTED AS A FUNCTION OF WAVELENGTH FOR VARIOUS ELECTRON TEMPERATURES AND DENSITIES[21]

K. L. Bowles[24] of the Jicamarca Radio Observatory in Peru has conducted several series of measurements in an attempt to obtain solar echoes at 50 Mc. No echoes were obtained even though the product of transmitter power and antenna gain is considerably greater than for any other solar radar system. This gives added evidence for a percipitous reduction of radar cross section with decreasing wavelength between 12 and 6 meters.

The second possible reason for the apparent cross section difference in the two experiments is the measured change in cross section with average solar activity. The 38 Mc results indicate that the average cross section has decreased steadily from 2.2 in 1961-62 to 0.6 photospheric areas in 1963-64[20]. The original 26 Mc data was taken in 1959, near the peak of the sunspot cycle. Since that time, several limited sets of measurements near 26 Mc have been made at Stanford, in the summer of 1962 and 1963. No detectable echoes were obtained even though the transmitter power is greater by 8 to 9 db than the 1959 system. There have been other changes in receiving and coding techniques, and also in the antenna system. In 1959, rhombic antennas were used at dawn, while the later experiments employed the log-periodic array near noon.

It does not appear possible at this time to be definite about the effects of frequency and solar activity from the various bits of evidence at hand. In view of the limited data taken on the lower frequency in 1959, it would appear that an understanding of these effects must await further experimentation, at least until the next period of maximum solar activity.

Even with the radar system in Texas, many minutes of signal integration are needed to demonstrate the presence of an echo. In order to obtain frequency and range-spread spectra, the integration of relatively strong returns is

required. It is not possible, unfortunately, to measure how the echo characteristics vary from second to second or even from minute to minute.

If a system were built with sufficient sensitivity to obtain reasonable S/N ratios without integration, the dynamic motion, shape, and echoing strength of the solar corona could be studied in considerable detail. Such a system would also be very useful for bistatic solar studies, and for both monostatic and bistatic radar studies of planetary ionospheres and surfaces. Planets and the interplanetary medium over essentially the whole of the solar system could be brought under intensive radar investigation with a combination of deep space probes and powerful transmitters and large antennas on the earth.

Acknowledgments

This report includes a brief review of some of the recent work at Stanford of my colleagues and students, in particular G. Fjeldbo, O. K. Garriott, H. T. Howard, B. B. Lusignan, F. L. Smith, III, and P. Yoh. Research support includes contracts from the National Aeronautics and Space Administration, the U. S. Air Force and Navy, and the National Science Foundation.

REFERENCES

1) V. R. Eshleman, P. B. Gallagher, and R. C. Barthle, J. Geophys. Research 65 (1960) 3079.

2) H. T. Howard, P. Yoh, and V. R. Eshleman, J. Geophys. Research 69 (1964) 535.

3) H. T. Howard, B. B. Lusignan, P. Yoh, and V. R. Eshleman, J. Geophys. Research 69 (1964) 540.

4) J. V. Evans and G. N. Taylor, Proc. Royal Soc. London, A., 263, (1961) 189.

5) C. G. Little and R. S. Lawrence, J. Research NBS, 64D, (1960) 335.

6) R. L. Smith, Jr., J. Geophys. Research 66(1961) 3209.

7) M. Neugebauer and C. W. Snyder, Science, 138 (1962) 1095.

8) D. L. Carpenter, private communication.

9) W. Priester, M. Roemer, and T. Schmidt-Haler, Nature 196 (1962) 464.

10) B. B. Lusignan, J. Geophys. Research 68 (1963) 5617.

11) The material in this section is based largely upon material being prepared for several publications by V. R. Eshleman, G. Fjeldbo, O. K. Garriott, and F. L. Smith, III.

12) G. Fjeldbo, Stanford University Dissertation (1964).

13) J. M. Kelso, Radio ray propagation in the ionosphere, (McGraw-Hill, New York, 1964) 237.

14) J. W. Chamberlain, Astrophys. J. 136 (1962) 582.

15) L. D. Kaplan, G. Munch, and H. Spinrad, Astrophys. J. 139 (1964) 1.

16) V. R. Eshleman, R. C. Barthle, and P. B. Gallagher, Science 131 (1960) 329.

17) R. C. Barthle, Stanford University Dissertation (1960).

18) W. G. Abel, J. H. Chisholm, P. L. Fleck, and J. C. James, J. Geophys. Research 66 (1961) 4303.

19) J. H. Chisholm and J. C. James, Astrophys.. J. (in press).

20) J. C. James, Trans. IEEE, PTGME (in press).

21) P. Yoh, Stanford University Report no. 2, contract AF 19(604)-7436 (1961).

22) C. W. Allen, Mon. Not. Roy. Astr. Soc. 107 (1947) 426.

23) D. E. Billings, Astrophys. J. 137 (1963) 592.

24) K. L. Bowles, private communication.